HHS Public Access

Author manuscript

Mol Carcinog. Author manuscript; available in PMC 2020 October 01.

Published in final edited form as:

Mol Carcinog. 2019 October ; 58(10): 1908–1918. doi:10.1002/mc.23084.

Targeting CCK2R for pancreatic cancer chemoprevention

Altaf Mohammed[1], **Naveena B Janakiram**[2,*], **Chen Suen**[1], **Nicole Stratton**[2], **Stanley Lightfoot**[2], **Anil Singh**[2], **Gopal Pathuri**[2], **Rebekah Ritchie**[2], **Venkateshwar Madka**[2], **Chinthalapally V Rao**[2]

[1]Division of Cancer Prevention, Chemoprevention Agent Development Research Group, National Cancer Institute, Bethesda, MD 20850, USA;

[2]Center for Cancer Prevention and Drug Development, Hem-Onc Section, Department of Medicine, Stephenson Cancer Center, University of Oklahoma Health Sciences Center, VA Medical Center, Oklahoma City, OK 73104, USA

Abstract

Gastrin signaling mediated through cholecystokinin-2 receptor (CCK2R) and its down-stream molecules is altered in pancreatic cancer. CCK2R antagonists, YF476 (netazepide) and JNJ-26070109, were tested systematically for their effect on pancreatic intraepithelial neoplasia (PanIN) progression to pancreatic ductal adenocarcinoma (PDAC) in $Kras^{G12D}$ mice. After dose selection using wild-type mice, six-week-old $p48^{Cre/+}$-LSL-$Kras^{G12D}$ (22–24/group) genetically engineered mice (GEM) were fed AIN-76A diets containing 0, 250, or 500 ppm JNJ-26070109 or YF-476 for 38 weeks. At termination, pancreata were collected, weighed, and evaluated for PanINs and PDAC. Results demonstrated that control-diet-fed mice showed 69% (males) and 33% (females) incidence of PDAC. Administration of low and high dose JNJ-26070109 inhibited the incidence of PDAC by 88% and 71% ($p<0.004$) in male mice and by 100% and 24% ($p>0.05$) in female mice, respectively. Low and high dose YF476 inhibited the incidence of PDAC by 74% ($p<0.02$) and 69% ($p<0.02$) in male mice and by 45% and 33% ($p>0.05$) in female mice, respectively. Further, transcriptome analysis showed downregulation of Cldn1, Sstr1, Apod, Gkn1, Siglech, Cyp2c44, Bnc1, Fmo2, 623169, Kcne4, Slc27a6, Cma1, Rho GTPase activating protein 18, and Gpr85 genes in JNJ-26070109-treated mice compared with untreated mice. YF476-treated mouse pancreas showed downregulation of Riks, Zpbp, Ntf3, Lrrn4, Aass, Skint3, Kcnb1, Dgkb, Ddx60, and Aspn gene expressions compared with untreated mouse pancreas. Overall, JNJ-26070109 showed better chemopreventive efficacy than YF476. However, caution is recommended when selecting doses, as the agents appeared to exhibit gender-specific effects.

Correspondence to: **Chinthalapally V. Rao,** Center for Cancer Prevention and Drug Development, Department of Medicine, Hem/Onc Section, University of Oklahoma Health Sciences Center (OUHSC), 975 NE10th St. BRC1207, Oklahoma City, OK 73104, USA Phone: 405-271-3224, Fax: 405-271-3225, cv-rao@ouhsc.edu.

*Current Address: Regenerative Biosciences Division, DoD/VA Extremity Trauma and Amputation Center of Excellence, Walter Reed National Military Medical Center, Bethesda, MD 20889

CONFLICTS OF INTEREST

The authors have no conflicts of interest.

Data Availability Statement: The data that support the findings of this study are available from the corresponding author upon reasonable request.

Keywords

CCK2R; Pancreatic Cancer; Chemoprevention; Kras

Introduction

Pancreatic ductal adenocarcinoma (PDAC) is a deadly disease with the least five-year survival among all cancer-related deaths. Almost 56,770 individuals will be diagnosed with PDAC, with ~45,750 deaths expected, in the US alone in 2019 (1). The lack of effective interventions is a major factor contributing to the poor prognosis and dismal survival rates of PDAC (2). Decades-long research in understanding pancreatic cancer biology and therapeutic intervention has led to minimum benefits despite the use of aggressive treatment modalities. Early detection at precancerous stages and chemoprevention offers enormous potential for increasing the survival and lowering the societal financial burden (3).

Like many other cancers, the development of PDAC from initial precursor lesions takes several years before it is diagnosed at advanced stages due to the lack of early signs and symptoms (2–5). Further, PDAC develops resistance to current therapies, leading to low survival. Although the exact reasons for this striking therapeutic resistance are unknown, many studies suggest that since this cancer is associated predominantly with Kras mutations and targeting Kras has proven to be difficult, these mutations may be the key to therapeutic resistance.

Since it is difficult to diagnose the disease at early stages, applying chemoprevention strategies to target PDAC is quite challenging. However, there are cohorts who might be at risk of developing PDAC during their lifetime who may be ideally suited to chemoprevention intervention. Individuals at high risk of the development of PC include those with i) genetic history (e.g., CDKN2A-p16-Leiden mutation, BRCA2 mutation, familial history); ii) early onset of diabetes in older individuals, smoking, and obesity; and iii) early lesions, such as PanINs, MCNs, and IPMNs (1). Hence, developing strategies that delay or prevent the formation and/or progression of pancreatic intraepithelial neoplasms (PanINs) to PDAC are of utmost importance.

Gastrin signaling mediated through gastrin/cholecystokinin-2 receptor (CCK2R) and its down-stream signal molecules is overexpressed in pancreatic cancers. In particular, CCK2R is highly expressed in PDAC stellate cells and is involved in fibrosis and PDAC progression (6–10). In the present study, we first confirmed the expression of key signaling molecules of CCK2R, such as RhoB/ROCK, RhoH, PIP2, DAG lipase, and Src, in genetically engineered $p48^{Cre/+}$-LSL-$Kras^{G12D/+}$ mouse (GEM) PDAC compared with normal pancreas (Supplementary Figure 1). Then, we evaluated the chemopreventive potential of two CCK2R antagonists, JNJ-26070109 and YF476, against pancreatic cancer using the GEM model.

Materials and Methods:

Agents:

CCK2R antagonists JNJ-26040109 and YF476 (netazepide) were supplied by the NCI DCP Repository/MRI Global Inc. (Kansas City, MO). YF-476 was stored at 4°C and JNJ-26040109 was stored at room temperature. The purity analysis was performed at the CCPDD Chemistry Core lab using NMR and HPLC.

Mouse model:

$P48^{Cre/+}$ and LSL-$Kras^{G12D/+}$ (C57BL/6 background) mice were bred and maintained under heterozygous conditions. Generation of $p48^{Cre/+}$-LSL$Kras^{G12D/+}$ mice expressing the activated KrasG12D oncogene has been described previously (11–13). We will henceforth refer to these mice as Kras mice or GEM. All animal research was performed under the animal protocols approved by the University of Oklahoma Health Sciences Center (OUHSC) Institutional Animal Care and Use Committee (IACUC). Animals were housed in ventilated cages under standardized conditions (21°C, 60% humidity, 12-h light/12-h dark cycle, 20 air changes/h) in the OUHSC rodent barrier facility. Mice were allowed ad libitum access to the respective diets and to automated tap water purified by reverse osmosis.

Experimental diets:

A semi-purified diet based on modified AIN-76A was used (Casein, 20%; Corn Starch, 52%; Dextrose, 13%; Corn oil, 5.0%; Alphacel/cellulose, 5.0%; *DL*-Methionine, 0.3%; Mineral mix AIN, 3.5%; Vitamin mix, AIN, 1.0%; and Choline bitartrate, 0.2%). All experimental diets were formulated and prepared at the research diet preparation core. All ingredients of the diet were purchased from the same source (Bioserv, NJ) throughout the study. All diets were mixed thoroughly so that all diet ingredients were uniformly distributed in the diet.

Determine the MTD of JNJ-26070109 and YF476 in mice:

At 7 weeks of age, male and female C57BL/6J mice (N=6/group) in each group received their respective control and experimental diets containing one of the five dose levels (0, 100, 200, 400, and 800 ppm) of JNJ-26070109 and YF476 until termination of the study after six weeks on experimental diets (Supplementary Table 1 & Supplementary Figure 2A). Body weights (Supplementary Figure 2B–E) and symptoms of toxicity were recorded weekly for six weeks. At termination, all organs were examined grossly for any abnormalities.

Bioassay Method for Efficacy Testing:

The experimental design to test the efficacy of JNJ-26070109 and YF476 is shown in Supplementary Table 2 and Figure 1A. After breeding the required quantities of Kras activated $Kras^{G12D/+}$ mice (male and female), at 5 weeks of age the mice were randomized and divided into the appropriate treatment groups consisting of 22–24 mice/group (Supplementary Table 2 and Figure 1A). As shown in Figure 1A, JNJ-26070109 and YF476 were administered by diet, beginning at the PanIN stage (6 weeks of age). All animals were weighed every week for the first 10 weeks, then every two weeks throughout the remainder

of the experiment. Mice at 44 weeks of age were weighed (Figure 1B–E) and then killed by CO_2 euthanasia. Pancreata were collected and weighed, and a small piece was snap-frozen in liquid nitrogen and stored in formalin. PanIN lesions and PDAC in collected pancreata were evaluated histopathologically. Efficacy endpoints were pancreatic tumor weights, PDAC incidence, PanIN lesion multiplicity (PanIN1, PanIN2, PanIN3), PDAC spread/normal pancreas, dose-response, and additive efficacy effects.

Positron emission tomography–computed tomography (PET-CT) imaging:

PET-CT imaging was performed on treated and untreated Kras mice (n=4) just before termination of the study to assess the progression or regression of PDAC. The methodology for PET-CT imaging has been well established in our core facility and details have been published (14). Briefly, positron emission tomography (PET) was performed by the Research Imaging Facility in the College of Pharmacy. Mice were fasted overnight prior to imaging. On the day of imaging, mice were anesthetized (2% isoflurane-air mixture) and injected with 100 μCi of FDG in the tail vein 11/2 hours before PET imaging. One hundred and twenty minutes after injection, the mice were re-anesthetized for imaging and positioned supine in a gantry of a PET-CT dual modality machine form Gamma Medica Ideas (Northridge, CA, USA). A fly-mode CT of the mouse body core was acquired before a 20-minute-long list-mode PET acquisition at 11/2 h post injection. Throughout the imaging period, the mice remained anesthetized. After imaging, the mice were allowed to wake up and were kept in their cage until the time of euthanasia. The acquired images were reconstructed by filtered back projection algorithm and fused with the CT image to generate a composite PET-CT image. The composite images were used for segmentation based drawing of 3D-regions of interest (ROI) using AMRIA 5.1 software (FEI, Hillsboro, Oregon 97124 USA).

Immunohistochemistry (IHC):

Five-μm fixed pancreas sections from control and treated mice were incubated with primary antibodies in a hybridization chamber for 1 h at room temperature or overnight at 4°C. The primary antibodies used were mouse-specific PCNA (Cat#SC-56, Lot#I1212), caspase3, Bcl2, and p21 (Santa Cruz, CA). Following incubation with the primary antibody, sections were incubated for 1 h with anti-mouse or anti-rabbit secondary antibodies, as appropriate for each primary antibody, then were visualized with diaminobenzidine (DAB) and counterstained with hematoxylin for IHC. Slides were observed under an Olympus microscope 1X701 and digital computer images were recorded with an Olympus DP70 camera.

Whole Transcriptome Analysis (WTA):

Next Generation Sequencing (NGS)-based WTA expression analysis was performed using an Illumina Miseq 2500 Next Generation Sequencer. Total RNA was extracted from the pancreatic tissues with a Totally RNA kit (Ambion), followed by mRNA purification (Ambion kit). The quality of the purified mRNA was tested with a Bio-analyzer (OUHSC Microgen core facility). Samples with an RNA integrity number (RIN) of 5 to 9 were sent for Next Generation Sequencing with Illumina at the OUHSC laboratory for genomics and bioinformatics Microgen core facility. The purified mRNA was converted to a cDNA library

and sequenced through the Illumina platform. Four to five million readouts were obtained, which was a comparable result to those in other recent publications on whole transcriptome analysis. At the Microgen Core Lab, cDNA was generated by reverse transcription from adaptors ligated to ends of the mRNA molecule. cDNA was amplified using primers complementary to adaptors and then purified by magnetic bead clean up method. After constructing cDNA libraries, cDNAs were amplified using standard emulsion PCR. After amplification, cDNA was deposited on beads on a slide for sequencing on the Illumina analyzer. The sequencing produced datasets of nucleotide sequence readouts. The readouts were analyzed with GeneSifter software (Geospiza; http://www.geospiza.com/), available at the Microgen core. Using the readouts/dataset, the software: 1) aligned transcriptome reads to a human genome, 2) counted tags for genes or exons, and 3) visualized the data.

Statistical Analysis:

Statistical analysis of the data are presented as Mean ± *SE*, or percentage of occurrence or average per group. These data were analyzed by GraphPad Prism Software 6.0. The total number of PDAC-bearing animals with respect to the total number of animals at risk in each group (carcinoma incidence or percentage mice with PDAC) were analyzed by two-tailed Fisher's Exact test. PDAC multiplicity (total number of invasive lesions per pancreas) and PanIN multiplicity (total number of non-invasive lesions per pancreas) were also calculated for each group (Mean ± *SE*), and the significance of the difference between the groups was analyzed by one-tailed *t*-test with Welch's correction.

Results:

MTD and the optimal dose of JNJ-26070109 and YF476:

MTD and optimal non-toxic dose studies on both CCK2R antagonists were performed using C57Bl/6 wild-type mice per the protocol (Supplementary Table 1 and Supplementary Figure 2A). Both YF476 and JNJ-26070109 were tested at different dose levels (0, 50, 100, 200, 400, and 800 ppm) to evaluate the toxicity. Based on the body weight gain and gross observations of all organs (liver, spleen, kidneys, pancreas), up to 800 ppm of both drugs had no effect on the body weight, and there were no external signs of toxicity or any changes in organ weights. As shown in Supplementary Figure 2B–E, there was no effect on body weight retardation after six weeks of drug administration in diet. Doses of 250 and 500 ppm were chosen for further evaluation to determine the chemoprevention efficacy in the $Kras^{G12D/+}$ GEM mice.

Chemopreventive efficacy of JNJ-26070109 and YF476 in $p48^{Cre/+}$-LSL-$Kras^{G12D/+}$ mice: General health of animals:

The experimental protocol for evaluating JNJ-26070109 and YF476 in pancreatic cancer progression is summarized in Figure 1A and Supplementary Table 2. Kras mice fed AIN-76A or JNJ-26070109 and YF476 diets had steady body weight gain. As shown in Figure 1B–E, there was no significant difference in body weight between the mice fed control AIN-76A diet and those fed AIN-76A diet supplemented with 250 ppm JNJ-26070109 or YF476, nor with 500 ppm of YF476. A significant body weight loss

(14.5%, $p<0.0015$) was observed in male animals fed 500 ppm of JNJ-26070109 (Figure 1B).

PET-CT imaging analysis:

PET-CT imaging was used to evaluate whether JNJ-26070109 and YF476 suppressed, regressed, or promoted pancreatic ductal adenocarcinoma formation. $Kras^{G12D/+}$ mice treated with both CCK2R antagonists were evaluated for the ability to suppress tumor growth through imaging at 44 weeks of age (Supplementary Figure 3). Representative images showing the effects of JNJ-26070109 and YF476 are shown in Supplementary Figure 2B and C, respectively. The PET-CT imaging did not show inhibition of tumor growth in treated animals compared with control animals. The agents might have not shown a significant inhibitory effect on PTs in the animals chosen for imaging, and, as seen after termination, the weights of the pancreatic tumors did not significantly decrease in the treatment groups.

Effect of JNJ-26070109 and YF476 on pancreatic tumor weight and PDAC incidence:

Pancreatic weight is a simple marker with which to assess the progression of tumors. The pancreatic weights of wild-type mice at 44 weeks of age were ~0.2–0.3 g. An increase in pancreatic weight (0.3 g to 2.7 g, a range across the groups) was observed in Kras mice (Figure 1F). As summarized in Figure 2, treatment of Kras male and female mice with 250 ppm of JNJ-26070109 or either dose of YF476 had little or no effect on the weight of pancreatic tumors; only treatment of male mice with 500 ppm of JNJ-26070109 caused a significant decrease (23.4%, $p<0.02$) in the weight of pancreatic tumors in GEM (Figure 2A). In control GEM, the mean pancreatic weights in males and females were 1.16 g and 0.92 g respectively (Figure 2A–D). In GEM fed 500 ppm JNJ-26070109, the mean pancreatic weights 0.89 g in males (Figure 2A). Histopathologic analysis of the pancreas using H&E-stained slides revealed no microscopic pathologic alterations in wild-type mice fed either AIN-76A or drug-supplemented diets. Control-diet-fed animals showed a 69% incidence of PDAC in males and 33% in females (Figure 2E–H). Dietary administration of low dose and high dose JNJ-26070109 inhibited incidence of PDAC 88% and 71% ($p<0.004$) in male mice and inhibited incidence of PDAC 100% and 24% (not significant, $p>0.05$) in female mice. Dietary administration of low dose and high dose YF476 inhibited the incidence of PDAC by 74% ($p<0.018$) and 69% ($p<0.02$) in male mice and by 45% and 33% (not significant, $p>0.05$) in female mice, respectively.

Effect of JNJ-26070109 and YF476 on PanIN lesion progression and % carcinoma.

Histological analysis showed 100% penetrance of pancreatic precursor PanIN lesions in the GEM fed AIN76A or drug-supplemented diets (Figure 3). The number of PanIN 1, 2, and 3 lesions in male GEM fed the control AIN76-A diet were (means ± S*EM*): 233 ± 32, 80 ± 8, and 41 ± 8, respectively; in the male mice fed 250 ppm JNJ-26070109, PanIN 1, 2, and 3 numbers were 189 ± 26, 52 ± 12, and 9 ± 5, respectively; and in male mice fed 250 ppm YF476 they were 277 ± 23, 78 ± 5, and 12 ± 5, respectively (Figure 3A and C). The number of PanIN 1, 2, and 3 lesions in male GEM fed the 500 ppm JNJ-26070109 were 168 ± 38, 50 ± 10, and 13 ± 10, respectively, and in the male mice fed 500 ppm YF476 were 243 ± 23, 53 ± 7, and 11 ± 16, respectively (Figure 3A and C).

The number of PanIN 1, 2, and 3 lesions in female GEM fed the control AIN76A diet were 156 ± 22, 76 ± 11, and 21 ± 7, respectively; in the female mice fed 250 ppm JNJ-26070109, the numbers were 236 ± 24, 53 ± 12, and 4 ± 3, respectively; and in female mice fed 250 ppm YF476, the numbers were 221 ± 42, 69 ± 12, and 9 ± 2, respectively (Figure 3B and D). The number of PanIN 1, 2, and 3 lesions in female GEM fed the 500 ppm JNJ-26070109 were 227 ± 42, 52 ± 11, and 10 ± 7, respectively, and in the female mice fed 500 ppm YF476 the numbers were 208 ± 43, 44 ± 12, and 16 ± 7, respectively (Figure 3B and D). The number of PanIN 3 lesions or carcinoma in situ was decreased in both drug-treated groups (Figure 3A–D).

Pancreata of male GEM fed AIN76-A diet showed a 15 ± 5% (Figure 3E and G) and female mice a 4 ± 3% (Figure 3F and H) cancer spread within the pancreata. The cancer spread % was decreased by JNJ-26070109 in male mice (Figure 3E). YF476 showed significantly reduced carcinoma spread in male mice (Figure 3G). Female GEM treated with a lower dose of JNJ-26070109 showed no carcinoma since there was no PDAC incidence, whereas a higher dose showed an increase in carcinoma spread (Figure 3F). Further, lower-dose YF476 treatment reduced carcinoma spread in female mice (Figure 3H).

Modulation of proliferation and apoptosis marker(s) by JNJ-26070109 and YF476 in pancreatic cancer.

The pancreatic tumor tissues obtained from male mice treated with JNJ-26070109 and YF476 were used to analyze the proliferation and apoptosis markers. IHC of PCNA, p21, Bcl2, and caspase3 markers was performed on untreated and treated PT tissues (Figure 4 A–D). Histological scoring provided by the pathologist found that the two agents had no significant effects of the levels of these markers, although there was a trend toward inhibition of proliferation by means of decrease in the expression of PCNA and an increase in the p21.

Modulation of CCK2R signaling biomarkers by JNJ-26070109 and YF476 in pancreatic cancer.

The pancreatic tumor tissues obtained from animals treated with JNJ-26070109 and YF476 were used to analyze the effects on various CCK2R-related signaling markers by next generation sequencing. Table 1 shows the number of upregulated and downregulated genes at different levels of expression. Table 2 and supplementary tables 3 and 4 show the list of altered genes in JNJ-26070109 and YF476, respectively. Tumors (including normal, preneoplastic lesions, and carcinoma) isolated from JNJ-26070109-treated mice showed downregulation of Cldn1, Sstr1, Apod, Gkn1, Siglech, Cyp2c44, Bnc1, Fmo2, 623169, Kcne4, Slc27a6, and Cma1, with alterations in expression ranging from 8.16- to 6.23-fold compared with tumor tissue isolated from control mice (Table 3). Rho GTPase activating protein 18, mRNA (1.39-fold), and Gpr88 (3.49-fold) were downregulated in tumors from JNJ-26070109-treated mice compared with tumor tissue isolated from untreated control animals (Supplementary Table 3). Tumor tissue isolated from YF476-treated mice showed downregulation of 4833403I15Rik, Zpbp, Ntf3, Lrrn4, Aass, 3632451O06Rik, Skint3, Kcnb1, 100043125, Dgkb, Ddx60, and Aspn with alterations in expression ranging from 7.3 to 4.61-fold compared with tumor tissue obtained from untreated control mice (Table 4).

YF476 transcriptome analysis showed upregulation of most of the Gpr and Rho signaling proteins, such as Gpr 162 (2.82 fold), Gprc5a (1.85 fold), Gpr125 (1.73 fold), and Gprc5d (1.51-fold), while only Mrgprb2 (2.68 fold) was observed to be downregulated (Supplementary Table 4). Table 2 shows a similar pattern with both drugs in terms of downregulation and upregulation of transcripts in tumors from drug-treated mice compared with those from untreated controls.

Discussion:

Gastrin signaling mediated through gastrin/cholecystokinin type B receptor (also known as cholecystokinin-2 receptor, CCK2-R, or CCK2R) may have an important role in pancreatic carcinogenesis. CCK2R is overexpressed in both human and animal PDACs. Many reports indicate that gastrin signaling is involved in pancreatic tumor cell proliferation (8,10,15). Recently, it has been shown that CCK2R is highly expressed in PDAC stellate cells and is involved in fibrosis and PDAC progression (6–10). Consistent with other reports, transcriptomic analysis of $p48^{Cre/+}$-LSL-$Kras^{G12D/+}$ mouse pancreatic tumors that was conducted in our laboratory by Next Generation Sequencing showed an increased expression ($p<0.05$) of CCK2R relevant key signaling molecules, such as RhoB/ROCK, RhoH, PIP2, DAG lipase, and Src, in pancreatic ductal adenocarcinoma (PDAC) compared with the normal pancreas (Supplementary Figure 1).

Stimulated by natural ligands, cholecystokinin 2 receptor (CCK2R) signaling regulates the physiological and pathophysiological functions in many tissues, and its effects are also seen in pancreatitis and PDAC (9,10). CCK2R signaling can lead to pancreatic fibrosis (9,10). Patients with chronic pancreatitis showed high levels of CCK (16–18). CCK2R-dependent signaling molecules RhoB/ROCK, RhoH, PIP2, DAG lipase, Src, and αV integrin were overexpressed in pancreatic cancer. Previously, it was shown that overexpression of αV integrin, Rho, PI3K/Akt, and several inflammatory molecules has a positive association with progression of pancreatic tumorigenesis in GEM (19–23). Several CCK2R antagonists, including JNJ-26070109, YM022, Z-360, and YF476 (netazepide), have been tested *in vitro* and in *in vivo* rodent models, and are in various stages of clinical development (21, 24–32). Similar to above observations, previously Smith et al (33) reported that CCK antagonist proglumide significantly inhibited PanIN 1 lesion progression to PanIN 3 and PanIN associated fibrosis in $Pdx1^{Cre}$.LSL-$KRas^{G12D}$ mice. Thus, targeting CCK2R for pancreatic chemoprevention appears to be a valid approach to PDAC prevention.

In the present study, to target CCK2R, two CCK2R antagonists, JNJ-26070109 and YF476, were tested for optimal dose (up to 800 ppm) and pharmacodynamic efficacy at two doses (250 and 500 ppm) for their effect on PanINs and their progression to PDAC in Kras mice. Six weeks of chronic administration to find the optimal dose did not show any significant changes in body weights and/or any overt toxicities. In the chemopreventive efficacy study, control-diet-fed mice showed a 69% incidence of PDAC in male mice. Dietary JNJ-26070109 and YF476 significantly inhibited PDAC incidence in male GEM. Female mice showed a lower incidence of PDAC (33%), and only the low dose of JNJ-26070109 was able to significantly reduce the incidence of PDAC. Both agents showed inhibition of PanIN2 and 3 in male mice, albeit to a lesser extent in female mice. PET-CT imaging was

performed on male animals from the high dose and low dose JNJ-26070109 treatment groups and the high dose YF476 treatment group. PET-CT imaging analysis showed a trend towards decreased tumor growth in the low dose JNJ-26070109 treatment group (Supplementary Figure 3). The carcinoma spread in untreated male mice was 15% compared with 1.2–0.8% in the YF476 treatment group (Figure 3G). The carcinoma spread was lower in pancreatic tumor samples from female mice that received a low dose of either agent (Figures 3F and 3H). Notably, 100% inhibition of carcinoma spread was observed in JNJ-26070109-treated female mice (Figure 3F). However, efficacy results did not show clear dose-response effects. One possible reason might be that drug dosing based on the MTD/toxicity studies may not always provide optimal doses required for the CCK2R optimal inhibition. Also, higher dose of JNJ-26070109 showed a significant reduction in body weight gain indicating that there may some toxicities associated upon long-term administration of this drug. Thus, it is possible that an even lower dose (<250 ppm) might have provided better efficacy. Other reasons, such as drug off-target at higher doses, may be a limiting factor for lack of dose-response effects. Overall, histopathological observations support inhibition of PanIN progression to PDAC, with an inhibition of carcinoma in situ and reduction in the multiplicity of PanIN 3 lesions by low doses of JNJ-26070109 (Figure 3).

To understand part of the mechanism, levels of proliferation and apoptosis makers (PCNA, p21, caspase-3, and Bcl2) were analyzed by IHC. The results suggest a trend towards the inhibition of tumor cell proliferation (Figure 4). Rho GTPases are involved in cell cytoskeleton organization, migration, and transcription (34). NGS analysis of tumors with JNJ-26070109 treatment showed significant inhibition of Rho GTPase activating protein in treated tumors (Supplementary Figure 1). JNJ-26070109 also decreased expression of apolipoprotein interacting with the lipid transport mechanism, and somatostatin receptor 1, which regulates the somatostatin hormone signaling that is involved in anti-depressant actions. Gastrokine 1, which maintains mucosal integrity, was also decreased by JNJ-26070109 in treated tumors. JNJ-26070109 mostly showed decreased effects on various molecules that play a role in numerous functions related to cell junctions and transport (Tables 2, 3, and Supplementary Table 3). YF476 showed significant inhibition of molecules related to the lysine degradation pathway, memory, sensory neurons, sperm morphogenesis, and potassium voltage gated channel (Tables 2,4 and Supplementary Table 4). How/whether these molecules are involved in tumorigenesis and how the CCK2R antagonists modulate the relevant pathways and signaling molecules must be investigated. In conclusion, targeting the CCK2R pathway with JNJ-26070109 and, to a somewhat to a lesser extent, with YF476 showed chemopreventive effects in suppression of PDAC. Targeting the gastrin signaling pathway (CCK2R) for tumor inhibition may be an appropriate approach that may prevent pancreatic tumor progression and increase survival rates.

Supplementary Material

Refer to Web version on PubMed Central for supplementary material.

Acknowledgements

This work was supported by NCI-CN25001–26. Transcriptome analysis was in part supported by the National Center for Research Resources and the National Institute of General Medical Sciences of the National Institutes of Health through Grant Number 8P20GM103447.

Abbreviations:

CCK2R	cholecystokinin-2 receptor
DAG lipase	Diacyl glyceride lipase
GEM	Genetically engineered mouse
JNJ-26070109	(R)4-bromo-N-[1-(2,4-difluoro-phenyl)-ethyl]-2-(quinoxaline-5-sulfonylamino)-benzamide
PDAC	pancreatic ductal adenocarcinoma
PanIN	pancreatic intraepithelial neoplasms
PET-CT	Positron emission tomography-computed tomography imaging
YF476 (Netazepide)	(R)-1-[2,3-dihydro-2-oxo-1-pivaloylmethyl-5-(2’-pyridyl)-1H-1,4benzodiazepin-3-yl]-3-(3-methylamino-phenyl)urea

References:

1. American Cancer Society 2019. Atlanta, GA Cancer facts and figures 2019.
2. Mohammed A, Janakiram NB, Lightfoot S, Gali H, Vibhudutta A and Rao CV. Early Detection and Prevention of Pancreatic Cancer: Use of Genetically Engineered Mouse Models and advanced Imaging Technologies. Current Med Chem, 2012; 19(22):3701–3713.
3. Mohammed A, Janakiram NB, Madka V, Li M, Asch AS, Rao CV. Current Challenges and Opportunities for Chemoprevention of Pancreatic Cancer. Current medicinal chemistry. 2018; 25(22):2535–2544. [PubMed: 28183260]
4. Mazur PK, Siveke JT. Genetically Engineered mouse models of pancreatic cancer:Unravelling tumor biology and progressing translational oncology. Gut, 2011, Doi:10.1136/gutjnl-2011-300756.
5. Yachida S, Jones S, Bozic I, Antal T, Leary R, Fu B, Kamiyama M, Hruban RH, Eshleman JR, Nowak MA et al. Distant metastasis occurs late during the genetic evolution of pancreatic cancer. Nature, 2011; 467:1114–17.
6. Smith JP, Fantaskey AP, Liu G and Zagon IS. Identification of gastrin as a growth peptide in human pancreatic cancer. Am J Physiol 1995; 268: R135–R141. [PubMed: 7840313]
7. Smith JP, Liu G, Soundararajan V, McLaughlin PJ and Zagon IS. Identification and characterization of CCK-B/gastrin receptors in human pancreatic cancer celllines. Am J Physiol 1994; 266: R277–R283. [PubMed: 8304551]
8. Smith JP, Shih A, Wu Y, McLaughlin PJ and Zagon IS. Gastrin regulates growth of human pancreatic cancer in a tonic and autocrine fashion. Am J Physiol 1996; 270: R1078–R1084. [PubMed: 8928909]
9. Berna MJ, Seiz O, Nast JF, Benten D. et al. CCK1 and CCK2 Receptors are expressed on pancreatic stellate cells and induce collagen production. J. Biol. Chem, 2010; 285, 38905–38914. [PubMed: 20843811]

10. Dockray GJ, Moore A, Varro A, and Pritchard DM. Gastrin Receptor pharmacology. Curr. Gastroenterol Rep, 2012; 14, 453–459. [PubMed: 22983899]
11. Mohammed A, Janakiram NB, Brewer M, Ritchie RL, Marya A, Lightfoot S, Steele VE, Rao CV. Antidiabetic Drug Metformin Prevents Progression of Pancreatic Cancer by Targeting in Part Cancer Stem Cells and mTOR Signaling. Transl Oncol. 2013;6:649–659. [PubMed: 24466367]
12. Mohammed A, Janakiram NB, Madka V, Ritchie RL, Brewer M, Biddick L, Patlolla JM, Sadeghi M, Lightfoot S, Steele VE, Rao CV. Eflornithine (DFMO) Prevents Progression of Pancreatic Cancer by Modulating Ornithine Decarboxylase Signaling. Cancer Prev Res. 2014;7:1198–1209.
13. Rao CV, Janakiram NB, Madka V, Devarkonda V, Brewer M, Biddick L, Lightfoot S, Steele VE, Mohammed A. Simultaneous targeting of 5-LOX-COX and EGFR blocks progression of pancreatic ductal adenocarcinoma. Oncotarget. 2015; 6(32):33290–305. [PubMed: 26429877]
14. Rao CV, Mohammed A, Janakiram NB, Qian L, Ritchie RL, Lightfoot S, Vibhudutta A and Rao CV. Inhibition of Pancreatic Intraepithelial Neoplasia Progression to Carcinoma by Nitric Oxide–Releasing Aspirin in p48Cre/+–LSL-KrasG12D/+ Mice. Neoplasia, 2012;14(9):778–787. [PubMed: 23019409]
15. Fino G, Matters L,. McGovern C,. Gilius E, Smith JP. Down-regulation of the CCK-B Receptor in pancreatic cancer cells blocks proliferation and promotes apoptosis. Am J.of Physiol-Gastrointestinal and Liver Physiology. 2012; 302; G1244–G1252.
16. Slaff JI, Wolfe MM, Toskes PP. Elevated fasting cholecystokinin levels in pancreatic exocrine impairment: evidence to support feedback regulation. J Lab Clin Med 1985; 105: 282–5. [PubMed: 3973464]
17. Garcés MC, Gómez-Cerezo J, Alba D, et al. Relationship of basal and postprandial intraduodenal bile acid concentrations and plasma cholecystokinin levels with abdominal pain in patients with chronic pancreatitis. Pancreas 1998; 17: 397–401. [PubMed: 9821182]
18. Lieb JG II. Forsmark CE. Review article: pain and chronic pancreatitis. Aliment Pharmacol Ther29, 706–719. [PubMed: 19284407]
19. Kato H, Seto K, Kobayashi N, et al. CCK2/gastrin receptor signaling pathway is significant for gemcitabine-induced gene expression of VEGF in pancreatic cancer cells. Life Sci. 2011; 89, 603–608. [PubMed: 21839751]
20. Cayrol C, Bertrand C, Kowalski Chauvel A, et al., Alpha integrin: a new gastrin target in human pancreatic cancer cells. World J Gastroenterol, 2011; 17, 4488–4495. [PubMed: 22110279]
21. Berna MJ, Tapia JA, Sanchi V, Jensen RT. Progress in developing CCK/Gastrin receptor ligands that have therapeutic potential. Curr. Opin Pharmacol. 2007; 7, 583–592. [PubMed: 17997137]
22. Mohammed A, Qian L, Janakiram NB, Lightfoot S, Steele VE and Rao CV. Atorvastatin delays progression of pancreatic lesions to carcinoma by regulating PI3/AKT signaling in p48Cre/1 LSL-KrasG12D/1 mice. Internation J Cancer, 2012;131:1951–1962.
23. Mohammed A, Janakiram NB, Madka V, Brewer M, Ritchie RL, Lightfoot S, Kumar G, Sadeghi M, Patlolla JM, Yamada HY, Cruz-Monserrate Z, May R, Houchen CW, Steele VE, Rao CV. Targeting pancreatitis blocks tumor-initiating stem cells and pancreatic cancer progression. Oncotarget. 2015; 6(17):15524–39. [PubMed: 25906749]
24. Kidd M, Siddique ZL, Drozdov I, et al. The CCK(2) receptor antagonist,YF476, inhibits Mastomys ECL cell hyperplasia and gastric carcinoid tumor development. Regul Pept. 2010;162:52–60. [PubMed: 20144901]
25. Morton MF, Barrett TD, Freedman J, et al. JNJ-26070109 [(R)4-bromo-N-[1-(2,4-difluoro-phenyl)-ethyl]-2-(quinoxaline-5-sulfonylamino)-ben zamide]: a novel, potent, and selective cholecystokinin2 receptor antagonist with good oral bioavailability. JPharmacol Exp Ther. 2011;338:328–36. [PubMed: 21493750]
26. Akgun E, Korner M, Gao F, et al. Synthesis and in vitro characterization of radioiodinatable benzodiazepines selective for type 1 and type 2 cholecystokinin receptors. J Med Chem. 2009;52:2138–47. [PubMed: 19271701]
27. Patent WO201312679A1 Cholecystokinin B receptor targeting for imaging and therapy. Pages 1–39.
28. Murayama T, Matsumori Y, Ito M, et al., Antiproliferative effect of a novel cholescystokinin-B/gastrin receptor antagonist, YM022. Jap J. Cancer Res, 1996; 87, 743–750. [PubMed: 8698625]

29. Orikawa Y, Kato H, Seto K, et al. Z-360, a novel therapeutic agent for pancreatic cancer, prevents up-regulation of ephrin B1 gene expression and phosphorylation of NR2B via suppression of interleukin-1 beta production in a cancer-induced pain model in mice. Mol Pain. 2010;6:72. [PubMed: 20979661]

30. Jin G, Ramanathan V, Quante M, et al. Inactivating cholecystokinin-2 receptor inhibits progastrin-dependent colonic crypt fission, proliferation, and colorectal cancer in mice. J Clin Invest. 2009; 119(9):2691–2701. [PubMed: 19652364]

31. Meyer T, Caplin ME, Palmer DH, et al. A phase Ib/IIa trial to evaluate the CCK2 receptor antagonist in combination with gemcitabine in patients with advanced pancreatic cancer. Eur J Cancer. 2010;46:526–33. [PubMed: 20006921]

32. Grabowska AM, Morris TM, Kumari R, et al. Preclinical evaluation of a new orally-active CCK2R antagonist, in gastrointestinal cancer models. Regul Pept. 2008; 146, 46–57. [PubMed: 17961733]

33. Smith JP, Cooper TK, McGovern CO, Gilius EL, Zhong Q, Liao J, Molinolo AA, Gutkind JS, Matters GL. Cholecystokinin receptor antagonist halts progression of pancreatic cancer precursor lesions and fibrosis in mice. Pancreas, 2014; 47; 1050–1059.

34. Hodge Richard G. & Ridley Anne J.. Regulating Rho GTPases and their regulators. Nature Reviews Molecular Cell Biology 2016; 17(8):496–510. [PubMed: 27301673]

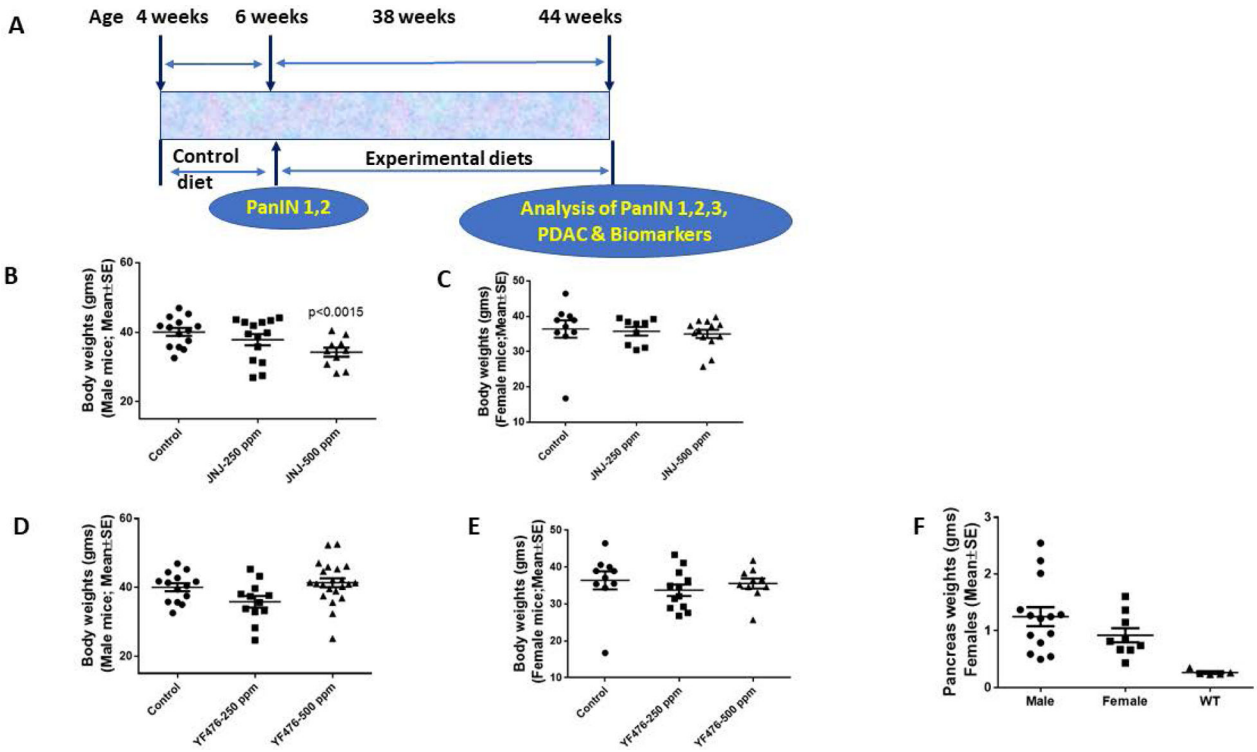

Figure 1.

A. Experimental design to evaluate the chemopreventive and dose-response effects of JNJ-26070109 and YF476 (YF-476) in $p48^{Cre/+}$-LSL-$Kras^{G12D/+}$ GEM. B. Effect of JNJ-26070109 on body weight gain of male GEM at 44 weeks. C. Effect of JNJ-26070109 on body weight gain of female GEM at 44 weeks. D. Effect of YF476 on body weight gain of male GEM at 44 weeks. E. Effect of YF476 on body weight gain of female GEM at 44 weeks. F. Pancreas weights of male and female GEM and wild-type mice at 44 weeks.

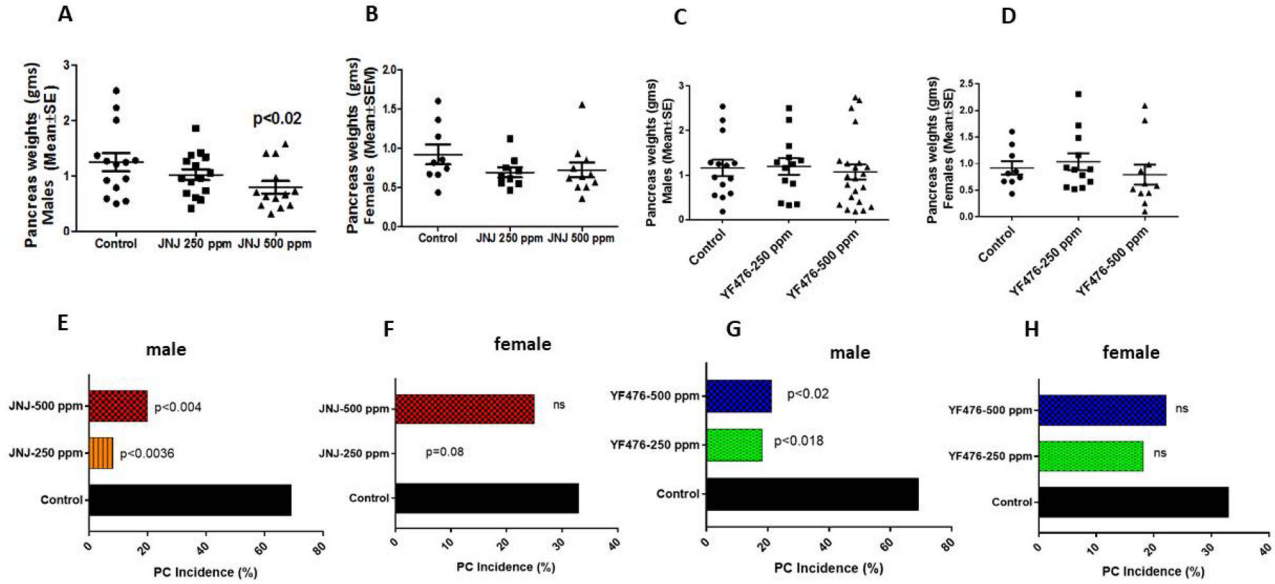

Figure 2.

Chemoprevention of pancreatic cancer by CCK2R antagonists. A. Pancreas weights of male GEM treated with JNJ-26070109 at 44 weeks of age. B. Pancreas weights of female GEM treated with JNJ-26070109 at 44 weeks of age. C. Pancreas weights of male GEM treated with YF476 at 44 weeks of age. D. Pancreas weights of female GEM treated with YF476 at 44 weeks of age. E. Effect of JNJ-26070109 on the incidence (percentage of mice with carcinomas) of pancreatic ductal adenocarcinoma in male GEM. F. Effect of JNJ-26070109 on the incidence (percentage of mice with carcinomas) of pancreatic ductal adenocarcinoma in female GEM. G. Effect of YF476 (netazepide) on the incidence (percentage of mice with carcinomas) of pancreatic ductal adenocarcinoma in male GEM. H. Effect of YF476 on the incidence (percentage of mice with carcinomas) of pancreatic ductal adenocarcinoma in female GEM.

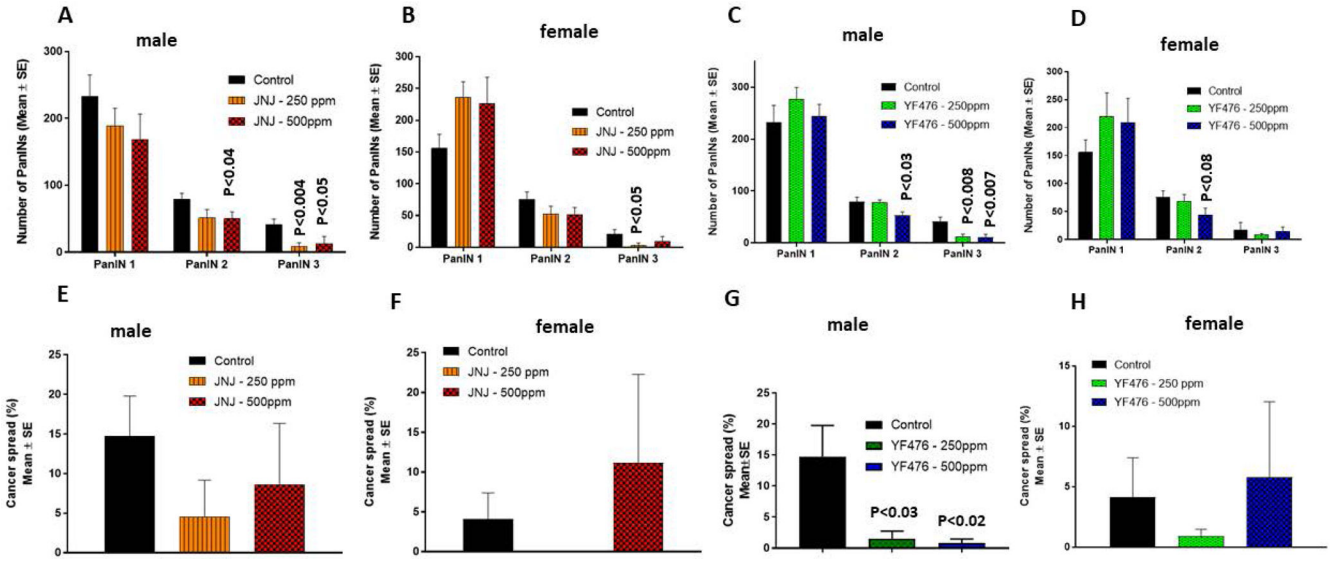

Figure 3.

Effect of CCK2R antagonists on PanIN multiplicity and carcinoma spread. A. Effect of JNJ-26070109 on the PanIN multiplicity in male GEM. B. Effect of JNJ-26070109 on the PanIN multiplicity in female GEM. C. Effect of YF476 on the PanIN multiplicity in male GEM. D. Effect of YF476 on the PanIN multiplicity in female GEM. E. Effect of JNJ-26070109 on the carcinoma spread in male GEM. F. Effect of JNJ-26070109 on the carcinoma spread in female GEM. G. Effect of YF476 (YF-476) on the carcinoma spread in male GEM. H. Effect of YF476 on the carcinoma spread in female GEM.

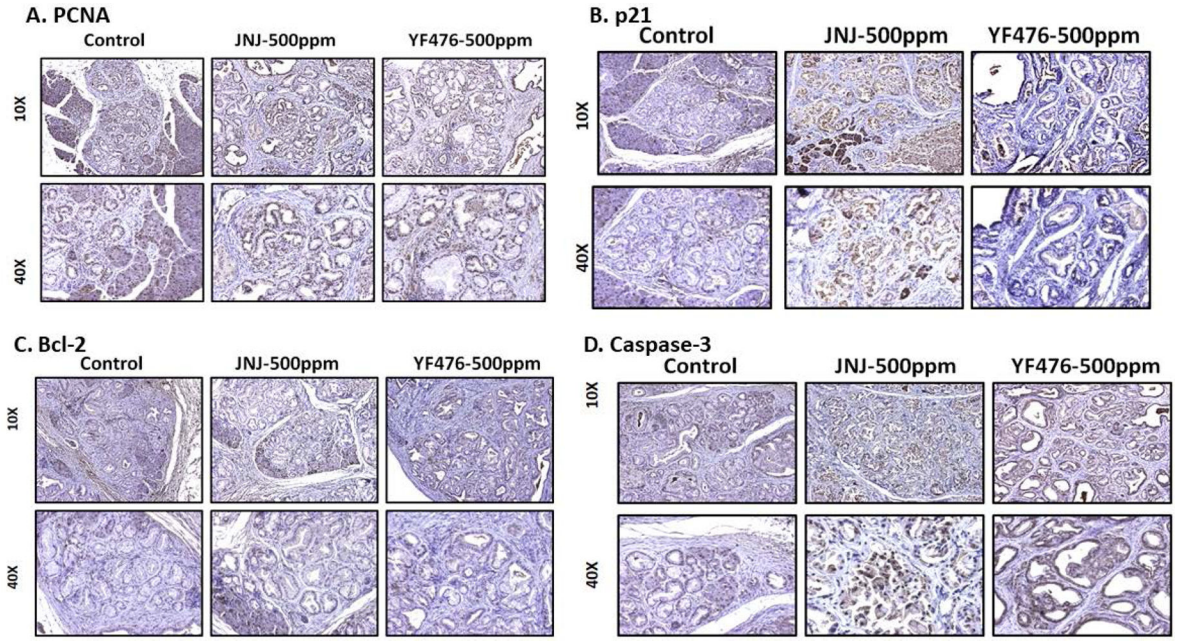

Figure 4.

Biomarker modulation by CCK2R antagonists in pancreatic tumors. A-J. Effect of JNJ-26070109 and YF-476 at 500 ppm on expression of PCNA (A), p21 (B), Bcl-2 (C), and caspase-3 (D) in pancreatic tumors from GEM.

Table 1:

Number of genes deregulated in pancreatic tumors treated with 500 ppm JNJ-26070109 and 500 ppm netazepide

Fold change	JNJ		Netazepide	
	UP	DOWN	UP	DOWN
<1.99	602	289	6866	232
<5	154	216	120	153
<10	21	22	7	12
>10	2	1	2	1
Total	779	528	6995	398

Table 2:

List of genes with similar gene expression patterns in both JNJ- and YF476-treated mouse pancreatic tumors (cutoff 2.5 fold)

JNJ		YF476				
Fold	***p*-value**	**Fold**	***p*-value**	**Direction**	**Gene Identifier**	**Gene Name**
2.72	0.0203	2.61	0.0335	**Down**	**Abca8a**	ATP-binding cassette, sub-family A (ABC1), member 8a (Abca8a), mRNA
2.86	0.0498	4.61	0.0296	**Down**	**Aspn**	Asporin, mRNA (cDNA clone MGC:41375 IMAGE: 1365428)
5.84	0.0020	2.78	0.0068	**Down**	**C7**	CDNA clone IMAGE:9007301
4.18	0.0272	4.69	0.0188	**Down**	**Ddx60**	DEAD (Asp-Glu-Ala-Asp) box polypeptide 60, mRNA (cDNA clone IMAGE:4037887)
2.77	0.0348	4.79	0.0121	**Down**	**Dgkb**	Diacylglycerol kinase, beta, mRNA (cDNA clone MGC: 99855 IMAGE:30649561)
4.64	0.0018	2.58	0.0042	**Down**	**Dio2**	Type II deiodinase
4.05	0.0290	3.02	0.0364	**Down**	**Dlg2**	Discs, large homolog 2 (Drosophila) (Dlg2), mRNA
3.21	0.0408	3.1	0.0422	**Down**	**Dpep1**	Dipeptidase 1 (renal), mRNA (cDNA clone MGC:6318 IMAGE:2812088)
3.43	0.0073	2.58	0.0266	**Down**	**Ecm2**	Extracellular matrix protein 2, female organ and adipocyte specific (Ecm2), mRNA
2.72	0.0054	2.82	0.0094	**Up**	**EG547267**	PREDICTED: Mus musculus predicted gene, EG547267 (EG547267), mRNA
2.95	0.0013	2.86	0.0372	**Up**	**ENSMUSG-000000–67783**	PREDICTED: Mus musculus similar to ribosomal protein L15, transcript variant 1 (LOC100043805), mRNA
3.97	0.0261	4.24	0.0269	**Down**	**Fgf7**	Fibroblast growth factor 7 (Fgf7), mRNA
5.11	0.0048	3.05	0.0120	**Down**	**Fgl2**	Fibrinogen-like protein 2, mRNA (cDNA clone MGC:19044 IMAGE:4189071)
3.5	0.0483	2.97	0.0440	**Down**	**Gabra3**	Gamma-aminobutyric acid (GABA-A) receptor, subunit alpha 3 (Gabra3), mRNA
4.5	0.0357	3.59	0.0435	**Down**	**Galntl2**	UDP-N-acetyl-alpha-D-galactosamine:polypeptide N-acetylgalactosaminyltransferase-like 2, mRNA (cDNA clone MGC:161357 IMAGE:40
4.85	0.0077	4.07	0.0133	**Down**	**GPDAC3**	Glypican 3, mRNA (cDNA clone MGC:35964 IMAGE: 4973409)
3.39	0.0206	3.14	0.0359	**Down**	**Ifit2**	Interferon-induced protein with tetratricopeptide repeats 2 (Ifit2), mRNA
3.16	0.0416	3.33	0.0032	**Down**	**Kcna6**	Potassium voltage-gated channel, shaker-related, subfamily, member 6 (Kcna6), mRNA
3.13	0.0422	5.13	0.0261	**Down**	**Kcnb1**	Potassium voltage gated channel, Shab-related subfamily, member 1, mRNA (cDNA clone MGC:25500 IMAGE: 4507847)
3.36	0.0119	2.58	0.0099	**Down**	**Klf14**	Kruppel-like factor 14 (Klf14), mRNA
3.98	0.0421	4.28	0.0447	**Down**	**Klf15**	Kruppel-like factor 15, mRNA (cDNA clone MGC:19125 IMAGE:4211067)
2.89	0.0286	2.98	0.0304	**Down**	**Klhl13**	Kelch-like 13 (Drosophila) (Klhl13), mRNA
2.57	0.0169	2.61	0.0408	**Down**	**Megf9**	Multiple EGF-like-domains 9, mRNA (cDNA clone MGC: 169753 IMAGE:8861148)
4.07	0.0085	3.18	0.0049	**Down**	**Olfml1**	Olfactomedin-like 1, mRNA (cDNA clone MGC:56882 IMAGE:6310165)

JNJ		YF476				
Fold	***p*-value**	**Fold**	***p*-value**	**Direction**	**Gene Identifier**	**Gene Name**
4.53	0.0317	3.05	0.0474	**Down**	**Pdgfd**	Platelet-derived growth factor, D polypeptide, mRNA (cDNA clone MGC:31518 IMAGE:4489485)
8.94	0.0056	8.93	0.0058	**Down**	**Pkhd1l1**	Polycystic kidney and hepatic disease 1-like 1 (Pkhd1l1), mRNA
4.16	0.0255	3.31	0.0482	**Down**	**Prlr**	Prolactin receptor, mRNA (cDNA clone MGC:6147 IMAGE:3500076)
2.67	0.0340	3.38	0.0161	**Down**	**Rora**	RAR-related orphan receptor alpha, mRNA (cDNA clone MGC:5892 IMAGE:3592667)
3.15	0.0007	3.44	0.0236	**Up**	**Rplp2**	Ribosomal protein, large P2, mRNA (cDNA clone MGC:6693 IMAGE:3583752)
3.8	0.0075	4.14	0.0196	**Down**	**Rprm**	Reprimo, TP53 dependent G2 arrest mediator candidate, mRNA (cDNA clone MGC:41066 IMAGE:1434823)
2.84	0.0015	2.62	0.0233	**Up**	**Rps17**	Ribosomal protein S17 (Rps17), mRNA
4.65	0.0053	3.05	0.0246	**Up**	**Snai3**	Snail-related zinc finger protein SMUC (Smuc)
3.1	0.0344	2.72	0.0149	**Down**	**Tceal1**	Transcription elongation factor A (SII)-like 1 (Tceal1), mRNA
3.98	0.0070	4.22	0.0076	**Down**	**Tcf21**	Transcription factor 21 (Tcf21), mRNA
3.42	0.0024	2.8	0.0128	**Down**	**Tlr11**	Toll-like receptor 11, mRNA (cDNA clone MGC:129352 IMAGE:40048069)
3.4	0.0250	2.68	0.0355	**Down**	**Tmeff2**	Transmembrane protein with EGF-like and two follistatin-like domains 2, mRNA (cDNA clone MGC:41091 IMAGE:1397175)
3.75	0.0053	11.22	0.0054	**Up**	**Ttn**	Titin, mRNA (cDNA clone IMAGE:5149168)
3.7	0.0041	2.75	0.0050	**Down**	**Zfp300**	Zinc finger protein 300 (Zfp300), mRNA

Table 3:

List of selected transcripts downregulated in JNF-26070109-treated pancreatic tumors compared with control group pancreatic tumors

Transcripts	Gene identifier	Fold change	Regulation
Gastrokine 2 (Gkn2), mRNA	Gkn2	8.16	Down
Claudin 1, mRNA (cDNA clone MGC:5767 IMAGE:3491319)	Cldn1	7.32	Down
Somatostatin receptor 1 (Sstr1), mRNA	Sstr1	7.23	Down
Apolipoprotein D (Apod), mRNA	Apod	7.14	Down
Gastrokine 1 (Gkn1), mRNA	Gkn1	6.97	Down
Sialic acid binding Ig-like lectin H, mRNA (cDNA clone MGC:178298 IMAGE:9053290)	Siglech	6.94	Down
Cytochrome P450, family 2, subfamily c, polypeptide 44, mRNA (cDNA clone IMAGE: 5097065)	Cyp2c44	6.6	Down
Basonuclin	Bnc1	6.58	Down
Flavin containing monooxygenase 2, mRNA (cDNA clone MGC:28212 IMAGE:3990305)	Fmo2	6.35	Down
ribosomal protein S17 pseudogene	623169	6.31	Down
Potassium voltage-gated channel, Isk-related subfamily, gene 4, mRNA (cDNA clone IMAGE:3470905)	Kcne4	6.29	Down
Solute carrier family 27 (fatty acid transporter), member 6 (Slc27a6), mRNA	Slc27a6	6.27	Down
Chymase 1, mast cell (Cma1), mRNA	Cma1	6.23	Down

Table 4:

List of selected transcripts downregulated in netazepide-treated pancreatic tumors compared with control group pancreatic tumors.

Transcripts	Gene identifier	Fold change	Regulation
PREDICTED: Mus musculus RIKEN cDNA 4833403I15 gene (4833403I15Rik), mRNA	4833403I15Rik	7.3	Down
Zona pellucida binding protein (Zpbp), mRNA	Zpbp	6.47	Down
Neurotrophin 3 (Ntf3), mRNA	Ntf3	6.31	Down
Neuronal leucine rich repeat-4	Lrrn4	6.04	Down
CDNA fis, clone TRACH2010974, highly similar to Mus musculus mRNA encoding lysine-ketoglutarate reductase/saccharopine dehydro	Aass	5.89	Down
RIKEN cDNA 3632451O06 gene, mRNA (cDNA clone MGC:32460 IMAGE:5043946)	3632451O06Rik	5.87	Down
Selection and upkeep of intraepithelial T cells 3 (Skint3), transcript variant 1, mRNA	Skint3	5.74	Down
Potassium voltage gated channel, Shab-related subfamily, member 1, mRNA (cDNA clone MGC:25500 IMAGE:4507847)	Kcnb1	5.13	Down
predicted gene 11711	1E+08	5.09	Down
Diacylglycerol kinase, beta, mRNA (cDNA clone MGC:99855 IMAGE:30649561)	Dgkb	4.79	Down
DEAD (Asp-Glu-Ala-Asp) box polypeptide 60, mRNA (cDNA clone IMAGE:4037887)	Ddx60	4.69	Down
Asporin, mRNA (cDNA clone MGC:41375 IMAGE:1365428)	Aspn	4.61	Down